INVESTIGATION OF MANIFOLDS IN THE CR3BP

Azem Hysa
Marsida Klemo

Applied and Natural Sciences Department,
"Aleksander Moisiu" University,
Durres, Albania

Abstract

The first aim of this paper is to find the locations of two Lagrange Points (LP) L_1 and L_2, calculate the Jacobi constant, to study the motion of a "test particle" inside the Earth-Moon system and then, the aim of this paper is to calculate and construct stable and unstable invariant manifolds through numerical iterative methods. We will present the results graphically and from these results we will give the appropriate explanations as to how a test body moves under the action of the gravitational field of two other massive bodies, such as Earth and Moon.
First, two periodic orbits around the two Lagrange points L_1 and L_2 are calculated. Then, in relation to these orbits, we have constructed the respective manifolds by making the careful choice of the initial conditions.
Manifolds are used in different fields and have many important applications. In the field of Mechanics of Celestial Bodies and Astrodynamics, they are mainly used to better understand how the trajectory of a test celestial body in space would be.
From many numerical tests, we found the appropriate initial conditions for the problem under consideration and then using the corresponding algorithm and writing the code in the MATLAB software, we have managed to find the Periodic Orbits (PO) and construct the stable and unstable manifolds of these orbits.

Keywords: Invariant Manifolds, Lagrange Points (LP), Periodic Orbits (PO), Earth-Moon system, MATLAB software.

1. Introduction

Throughout time and up to the present day, humanity has always been curious about the space beyond the planet in which we live, Earth. People are curious about how we can get to other bodies in space. The Sputnik 1 (an artificial satellite) was the first and most famous satellite launched from Earth in human history. This satellite was launched by the former Soviet Union in 1957 (Bertachini et al., 2013). This was a very important step for science in particular and humanity in general. Then, with the further development of space missions, human reached the Moon for the first time in 1969 (Bertachini et al., 2013). Today, many techniques are focused on the investigation and design of the artificial satellite's trajectories, spacecraft trajectories and space telescopes. To realize this objective, one of the techniques is through the invariant manifolds of CR3BP (More A., Ober-Blöbaum S., & Marsden J., E., 2012). Many researchers have done research and studies about the method of manifolds. For example, in a publication presented by Trusdale, the method of invariant manifolds is used to analyze the path that the space telescope must follow to get to the Lagrange points (Trusdale, 2012). In his study, he analyzed asteroid mining in the Lagrange point L_2 for the Sun-Earth system, and the transition of matter from L_2 point to the Earth-Moon system (Trusdale, 2012). Some other authors such as Belbruno, Gidea and Topputo use the separatrix property of invariant manifolds of periodic orbits around the Lagrangian points and show that, under certain conditions, points on stable

manifolds are WSB points (Belbruno, Gidea and Topputo, 2010). The L_2 Lagrange point in the Earth-Moon system has been and continues to be of recent interest for space missions. Also, the L_1 point in this system is important. In general, these points are important for other systems within the solar system as well as outside it. The importance of the L2 point was discussed at the International Astronautical Congress (IAC) in Naples in October 2012 by space agencies such as NASA and Boeing.

Based on the fact that these points are important, in our study, we have focused only on these two points for the Earth-Moon system. Periodic orbits around these points are of particular importance. We have constructed these orbits and presented them graphically. Then, in relation to these orbits, we have constructed stable and non-stable invariant manifolds.

The remainder of this paper is organized as follows. Section 2 describes the materials and methods used in this study. We use a gravitational model of the circular restricted three-body problem and some numerical techniques, such as Runge – Kutta – Fehlberg (RKF 45). In section 3, we describe our results and discussion, and our conclusions are presented in section 4.

2. Materials and methods

Many of the problems studied by Physicists and Mathematicians have a non-linear nature. Most of these problems do not have a general analytical solution. One of these is the problem with many bodies, such as, for example, the movement of celestial objects.

In the standard three-body problem, three masses are in gravitational interaction with each other. Based on the second law and the law of the gravitation of Newton the Equations of motions for this system are (Newton, 1687; Curtis, 2014; James, 2006):

$$\begin{aligned} m_1\ddot{\mathbf{r}}_1 &= \frac{Gm_2(\mathbf{r}_2-\mathbf{r}_1)}{|\mathbf{r}_2-\mathbf{r}_1|^3}+\frac{Gm_3(\mathbf{r}_3-\mathbf{r}_1)}{|\mathbf{r}_3-\mathbf{r}_1|^3} \\ m_2\ddot{\mathbf{r}}_2 &= \frac{Gm_1(\mathbf{r}_2-\mathbf{r}_1)}{|\mathbf{r}_1-\mathbf{r}_2|^3}+\frac{Gm_3(\mathbf{r}_3-\mathbf{r}_2)}{|\mathbf{r}_3-\mathbf{r}_2|^3} \\ m_3\ddot{\mathbf{r}}_3 &= \frac{Gm_1(\mathbf{r}_1-\mathbf{r}_3)}{|\mathbf{r}_1-\mathbf{r}_3|^3}+\frac{Gm_2(\mathbf{r}_2-\mathbf{r}_3)}{|\mathbf{r}_2-\mathbf{r}_3|^3} \end{aligned} \quad (1)$$

The system of differential equations (2) is non-integrable, unlike the problem of two bodies which is integrable (Poincaré, 1890). This system of nonlinear differential equations is very sensitive to the initial conditions (Poincaré, 1890). We are interested in special solutions for this system. Restricted 3-Body Problem (R3BP) assume $m_3 = 0$ (two large masses m_1 & m_2 and one tiny one m_3) (Lagrange, 1772).

We assume that a "test particle" P of negligible mass moves under the gravitational influence of Earth – Moon with masses m_E and m_M, respectively. We assume that the two masses have circular orbits about their common center of mass and that they exert a force on the particle although the particle cannot affect the two masses (Murray and Dermott, 1999). The primaries have constant separation and the same angular velocity as each other and their common center of mass (Murray and Dermott, 1999). In this case we have the CR3BP, Circular Restricted Three-Body Problem (Szebehely, 1967; Murray and Dermott, 1999). The system is described in a rotating system, and mass is normalized with the mass parameter $\mu = m_2/(m_1 + m_2)$, where $m_1 > m_2 \gg m_p$. The normalized mass primaries are $\mu_1 = 1 - \mu$ and $\mu_2 = \mu$ and the time unit is such that the orbital period T of primaries equals 2π and angular velocity is $\omega = 1$ (Szebehely,

1967; Murray and Dermott, 1999; Lu, J., Lu, Q., and Wang, 2011). We define the coordinates of m_1 as $(x_1, y_1, z_1) = (-\mu_2, 0, 0)$ and the coordinates of m_2 as $(x_2, y_2, z_2) = (\mu_1, 0, 0)$. If the particle is located at (x, y, z), then the distance formula shows that the distances between the particle and the masses are (Murray and Dermott, 1999):

$$\begin{aligned} r_1 &= \sqrt{(x+\mu_2)^2 + y^2 + z^2} \\ r_2 &= \sqrt{(x-\mu_1)^2 + y^2 + z^2} \end{aligned}, \tag{2}$$

respectively.
Equations of motion of the CR3BP in the rotating coordinate system are:

$$\ddot{\mathbf{r}} + 2\begin{pmatrix} -v_y \\ v_x \\ 0 \end{pmatrix} = \left(\frac{\partial U}{\partial \mathbf{r}}\right)^T, \tag{3}$$

where **r** is the position vector in the CR3BP, and the components of velocity of a test particle are v_x, v_y, v_z, respectively to direction *x*, *y* and *z*, *U*-is the potential energy of the system.

The CR3BP had five equilibrium points. These points are known as Lagrange points. In this study we focus only on the two Legrange points L_1 and L_2. We determined the position of these two points using numerical method. For this, we used an iterative method (Newton's method) to find the approximate root of nonlinear equation. This method is a root-finding algorithm in numerical analysis. The locations of triangular Lagrange points L_4 and L_5 are calculated based on an exact solution. The integral of motion (Jacobi constant) in the CRTBP is defined by equation (Jacobi, 1863; Paul Ricord Griesemer, 2009):

$$C = 2U - \left(v_x^2 + v_y^2 + v_z^2\right) \tag{4}$$

This quantity is very important because it plays the role of energy in this problem and is the only known conserved quantity for the CR3BP (reference).
The system of equations of motion for CR3BP can be linearized in the form:

$$\dot{\mathbf{x}} = A\mathbf{x} + \text{Quadratic term}, \tag{5}$$

where

$$A = \frac{\partial \dot{\mathbf{x}}}{\partial \mathbf{x}} = \begin{pmatrix} \frac{\partial \dot{x}}{\partial x} & \frac{\partial \dot{x}}{\partial y} & \frac{\partial \dot{x}}{\partial z} & \frac{\partial \dot{x}}{\partial \dot{x}} & \frac{\partial \dot{x}}{\partial \dot{y}} & \frac{\partial \dot{x}}{\partial \dot{z}} \\ \frac{\partial \dot{y}}{\partial x} & \frac{\partial \dot{y}}{\partial y} & \frac{\partial \dot{y}}{\partial z} & \frac{\partial \dot{y}}{\partial \dot{x}} & \frac{\partial \dot{y}}{\partial \dot{y}} & \frac{\partial \dot{y}}{\partial \dot{z}} \\ \frac{\partial \dot{z}}{\partial x} & \frac{\partial \dot{z}}{\partial y} & \frac{\partial \dot{z}}{\partial z} & \frac{\partial \dot{z}}{\partial \dot{x}} & \frac{\partial \dot{z}}{\partial \dot{y}} & \frac{\partial \dot{z}}{\partial \dot{z}} \\ \frac{\partial \ddot{x}}{\partial x} & \frac{\partial \ddot{x}}{\partial y} & \frac{\partial \ddot{x}}{\partial z} & \frac{\partial \ddot{x}}{\partial \dot{x}} & \frac{\partial \ddot{x}}{\partial \dot{y}} & \frac{\partial \ddot{x}}{\partial \dot{z}} \\ \frac{\partial \ddot{y}}{\partial x} & \frac{\partial \ddot{y}}{\partial y} & \frac{\partial \ddot{y}}{\partial z} & \frac{\partial \ddot{y}}{\partial \dot{x}} & \frac{\partial \ddot{y}}{\partial \dot{y}} & \frac{\partial \ddot{y}}{\partial \dot{z}} \\ \frac{\partial \ddot{z}}{\partial x} & \frac{\partial \ddot{z}}{\partial y} & \frac{\partial \ddot{z}}{\partial z} & \frac{\partial \ddot{z}}{\partial \dot{x}} & \frac{\partial \ddot{z}}{\partial \dot{y}} & \frac{\partial \ddot{z}}{\partial \dot{z}} \end{pmatrix} \tag{6}$$

is the Jacobian of the system and x is a vector with six elements. The general analytical solution of the linearized equation (5) around the Lagrangian points L_1 and L_2 is:

$$\mathbf{x}(t) = e^{\lambda t}\mathbf{v}, \quad (7)$$

where λ dhe $\mathbf{v}$ are the eigenvalue and eigenvector (Strogatz, 1995).

In this study we use the method of invariant manifolds. Manifolds depend on periodic orbits around the Lagrange points and they can be computed with respect to these orbits (Trusdale, 2012).
The unstable invariant manifold (M_{joS}) of an orbit contains the set of all trajectories that the test particle could have if it were to undergo a perturbation somewhere in that orbit in the direction of the unstable eigenvector of the orbit. Similarly, the stable invariant manifold (M_S) of an orbit contains the set of all trajectories that the test particle can have, to asymptotically arrive at that orbit along the stable eigenvector of the orbit (Thurman, Worfolk, 1996; Parker & Anderson, 2013; Trusdale, 2012).
For a given state $\mathbf{x} = (x_1, x_2, x_3, x_4, x_5, x_6)$, of the periodic orbit around the Lagrange points, the stable and unstable manifold can be calculated from the linear approximation of the system, considering a small perturbation ε applied to **x** which becomes xs (resp. x_{joS}) and propagating the equations of motion backward (resp. forward) from xs (resp. x_{joS}), with: $x_S(t) = x(t) \pm \epsilon v_S$ and $x_{joS}(t) = x(t) \pm \epsilon v_{joS}$ (Parker & Anderson, 2013).
Also, we used some numerical methods such as the Runge-Kutta-Fehlberg (RKF 45) method (Fehlberg 1960; Fehlberg 1968; Fehlberg 1969) to achieve the objectives of this study. The codes were built and tested the to model the trajectories of a test particle using MATLAB.

3. Results and discussions

The results of this study come from the numerical calculations of the system of nonlinear differential equations of the second order for the CRTBP model. These numerical calculations were performed in the MATLAB software, from which the results are displayed graphically. This is one of the most powerful software for the quality of the results presented graphically. Some results are presented in the (x, y) plane and others in the (x, y, z) space.
To generate the results, we consider the motion of a test particle in the *x – y* planes or in the space (*x, y, z*).
The mass ratio for the Earth – Moon system was assumed to be $\mu = 0.01215$. Using this value, we calculated the positions of the Lagrange points and the value of the Jacobi constant for each of these positions. $L_1 = L_1(x, y, z) = (0.8369, 0, 0)$, $L_2 = L_2(x, y, z) = (1.1557, 0, 0)$, $C_{L_1} = 3.1883$ $C_{L_2} = 3.1722$.
Figure 1 shows the position of the five Lagrangian points L_1, L_2, L_3, L_4, and L_5, respectively. Planet Earth is the blue globe and the Moon is the black dot. The trajectory with green color is the Zero Velocity Curve (ZVC) for C=3.14. This trajectory defines the limits of the allowed zone and the forbidden zone of the test particle. The two black orbits that are difficult to distinguish in the Figure are the periodic orbits around the Lagrangian points L_1 and L_2. The initial conditions for these two orbits are respectively: for the periodic orbit around the point L1; x_{10}=0.869581001; x_{30}=0; x_{50}=-0.05000012; x_{20}=0; x_{40}=-Velo(C,x_{10},x_{30},x_{50}); x_{60}=0; and for the

periodic orbit x_{10}=1.1173275000001; x_{30}=0; x_{50}=-0.0300000012; x_{20}=0; x_{40}=Velo(C,x_{10},x_{30},x_{50}); x_{60}=0.

If a test material point would start from the position with coordinates (-3.53983, -0.00976768, 0.00330564) then it would move according to one of the sky-colored trajectories shown in Figure 1. Then it would move according to the corresponding stable direction with the stable eigenvector and it would end without being too perturbed periodic orbit around point L_2. This is a stable manifold and is marked with the symbol $M^J_{S,L2}$. Figure 2 shows the $M^J_{joS,L2}$ unstable manifold (set of trajectories in pink). This manifold shows the path along which the test material point would move in the unstable direction characterized by the unstable eigenvector. In Figure 3, two manifolds are presented, one is stable (the set of trajectories with sky color) and the other is not stable (the set of trajectories with pink color). These two manifolds are calculated in relation to the periodic orbit around the point L_1. The symbols of these manifolds are respectively $M^B_{S,L1}$ and $M^B_{joS,L1}$. If a spacecraft were to start from the point with coordinates (-0.728499, -0.0819635, 0.0624661), then it would follow the steady-state path shown by the sky-color manifold and arrive close to the point L_1 without being disturbed by external actions. Then it would orbit periodically around this orbit.

These manifolds that we explained above, together with four other manifolds in the area near the Moon, can be presented in a summarized way in space (x, y, z), as in Figure 4. The coordinates x, y, and z are dimensionles. The two stable manifolds near the Moon are shown in blue, while the two non-stable manifolds are in red. Since these manifolds are not clearly distinguished in this summary figure, then we present it enlarged in the (x, y) plane. Here we clearly see these stable and non-stable trajectories. These manifolds are marked with symbols $M^g_{S,L1}$, $M^g_{S,L2}$ and $M^g_{joS,L1}$, $M^g_{joS,L2}$, respectively.

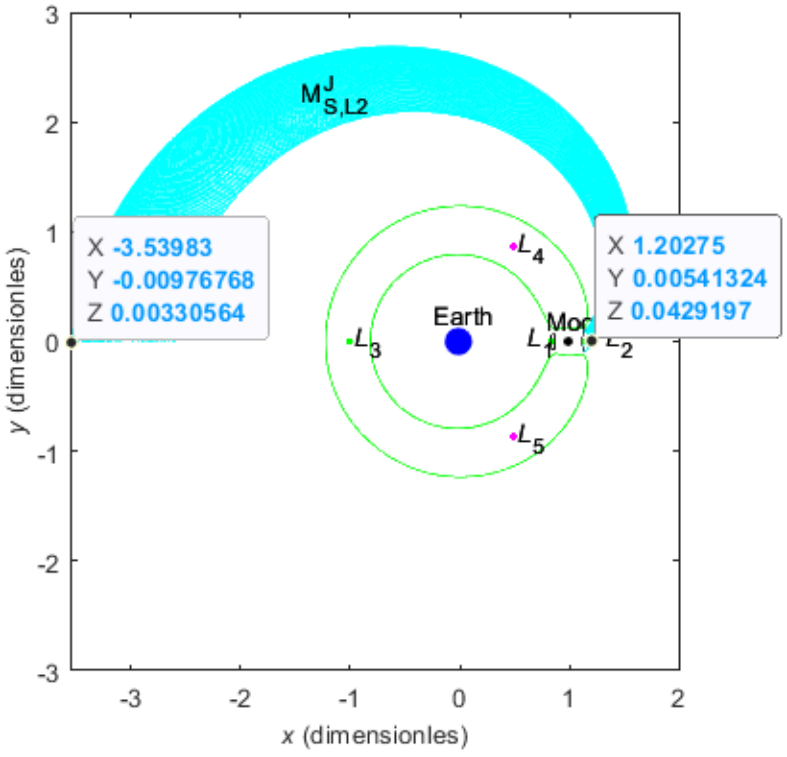

Figure 1. The stable invariant manifold associated with the periodic orbit around the Lagrangian point L_2.

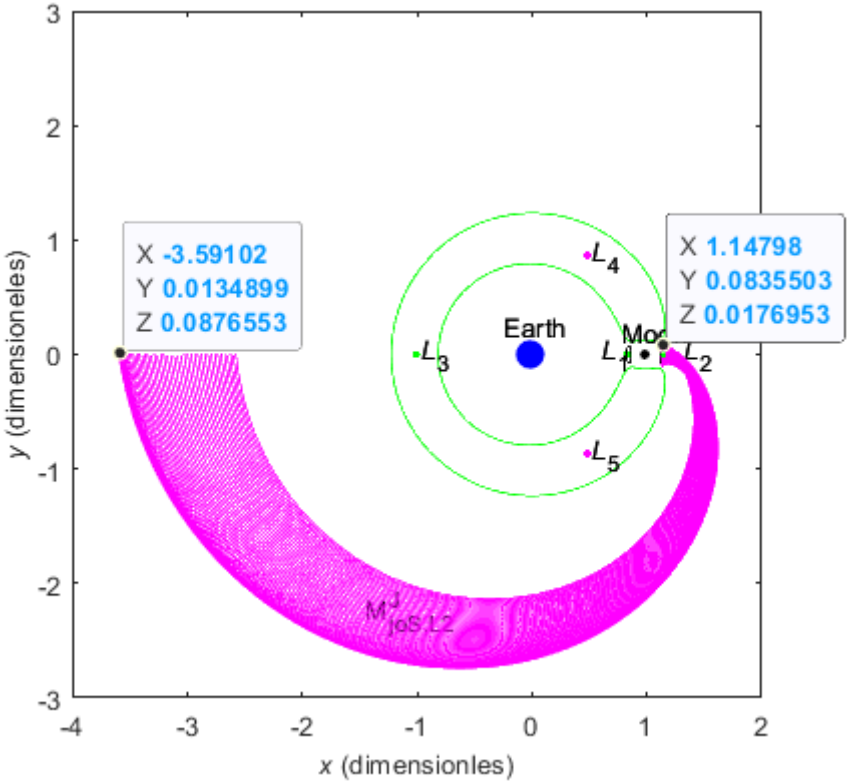

Figure 2. An unstable invariant manifold.

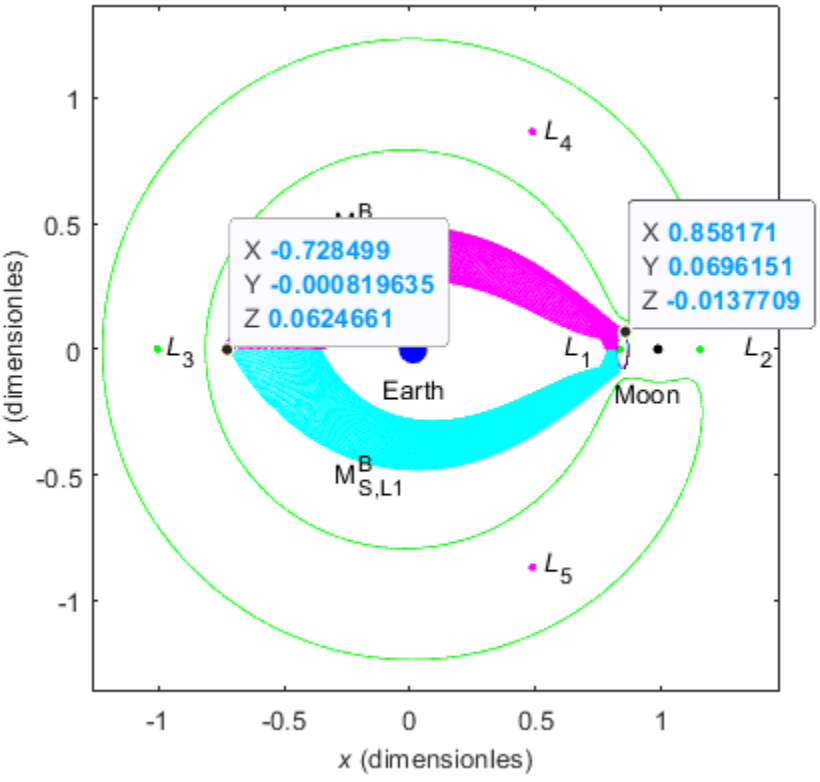

Figure 3. Two manifolds calculated in relation to the periodic orbit around the point L_1. The sky-colored trajectories represent the stable manifold and the pink ones non-stable.

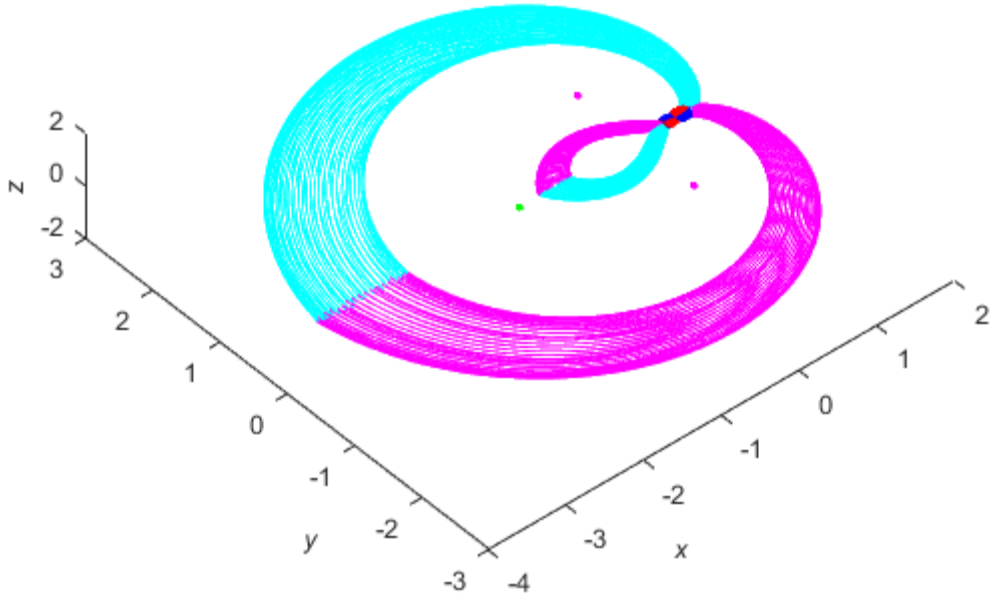

Figure 4. Eight stable and non-stable manifolds in the Earth-Moon system in space. The set of orbits with blue color and color-sky color are stable, while those with pink and red color are not stable.

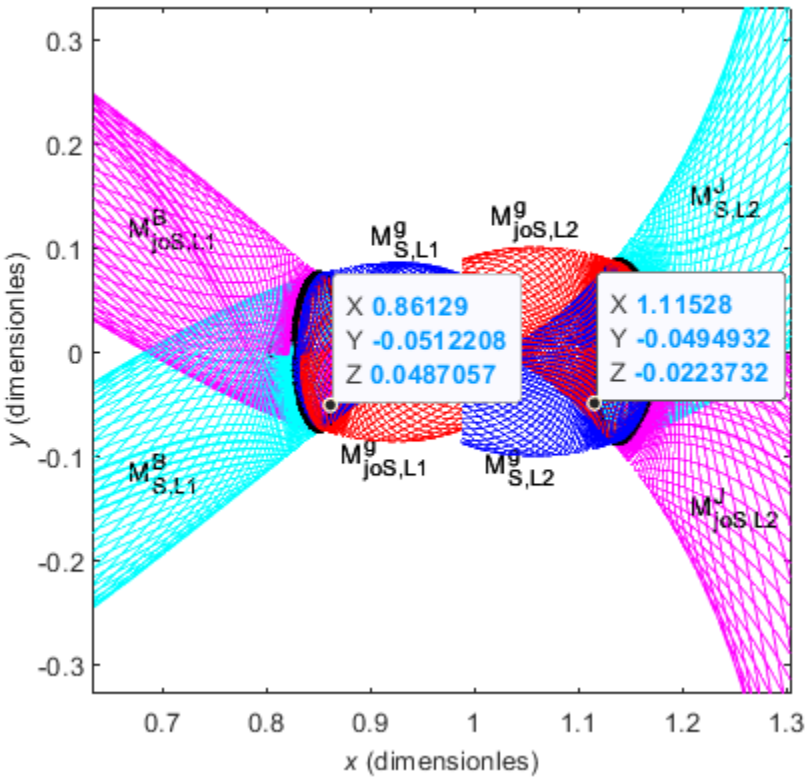

Figure 5. The manifolds of Figure 4 are presented in an enlarged manner near the Moon and two periodic orbits around points L_1 and L_2. In this case, the result is presented in the plan in such a way that it can be seen clearly.

The color-sky trajectory presented in Figure 6 is the trajectory of a test particle in the Earth-Moon system. In this result, the Earth is represented by a blue globe, the Moon by a black globe and point L_1 by a green square. Initial conditions for the coordinates and velocity of the test particle in this case are: $x_0 = 0.8000012$ (this is initial position near L_1); $y_0 = 0$; $z_0 = 0$; $v_{x0} = 0$ (this is the initial velocity according to direction x); $v_{y0} = 0.19999$ (this is the initial velocity near the manifold) and $v_{z0} = 0$. While Figure 7 shows the trajectory (in blue) of a test particle in the Sun-Earth system with initial conditions: $x_0 = 0.8500120134$; $y_0 = 0$; $z_0 = 0$; $v_{x0} = 0$; $v_{y0} = 0.10000120032$ and $v_{z0} = 0$. The result is presented in Cartesian space (x, y, z) in astronomical units. In this result, the Sun appears with a yellow globe and the Earth with a green globe. While point L1 in the Sun-Earth system is represented by a black square. The final result of this work is presented in Figure 8. This Figure represents an unstable manifold in the Sun-Earth system (Trajectory in pink) in the cartesian space (x, y, z). Again, in this case, Cartesian coordinates are presented in astronomical units.

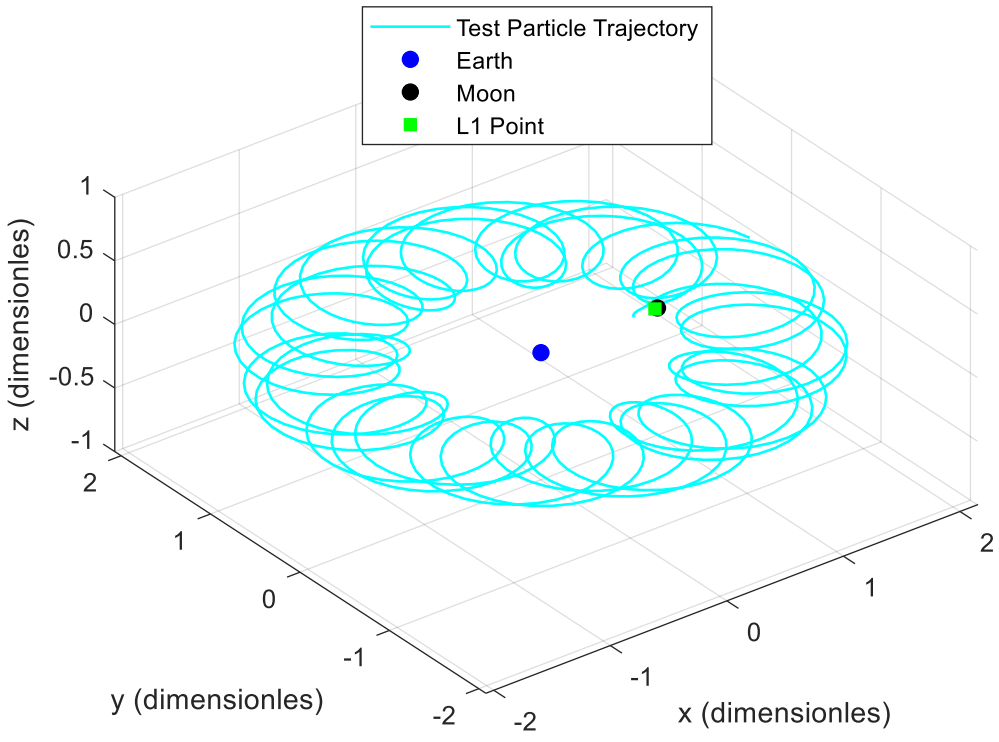

Figure 6. Test Particle Trajectory in CR3BP for $\mu = 0.01215$.

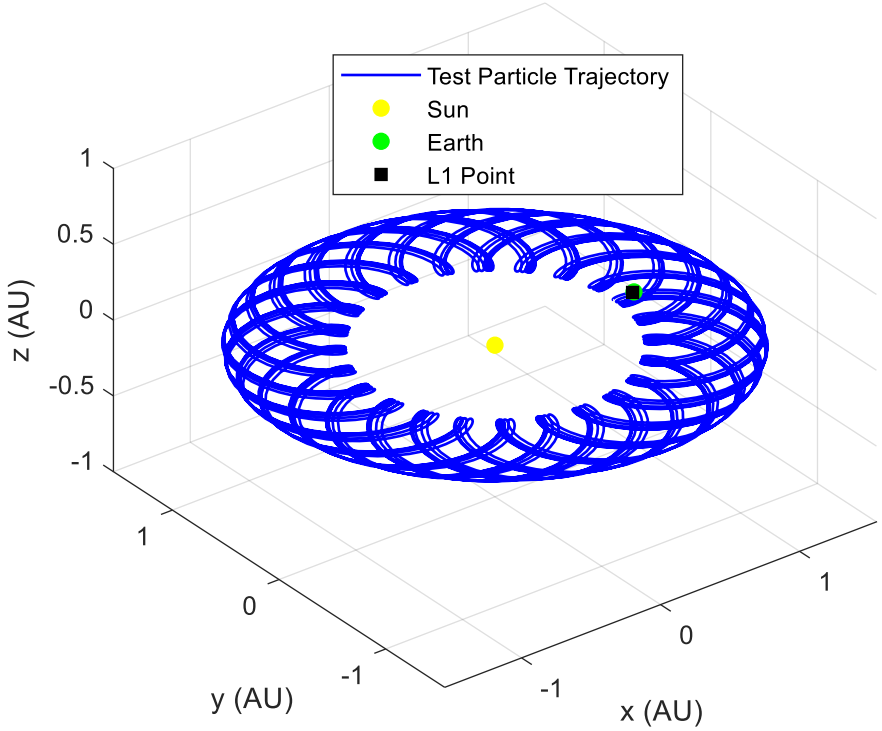

Figure 7. Test Particle Trajectory in CR3BP for $\mu = 3.35 \times 10^{-6}$. This value correspond with the mass parameter of the Sun-Earth system.

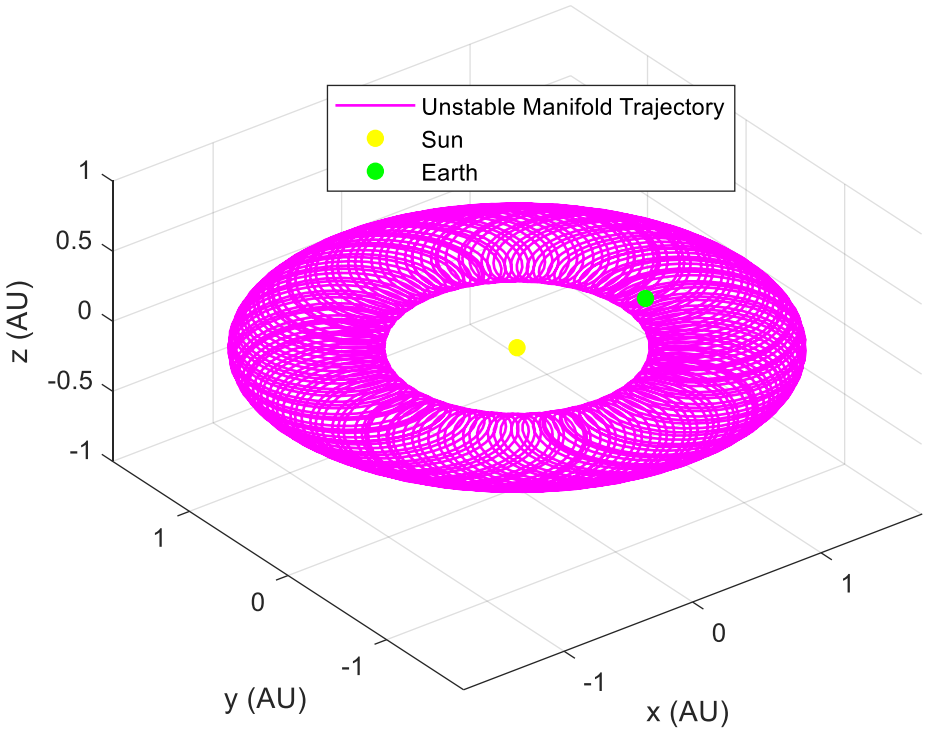

Figure 8. Unstable Manifold in CR3BP for the Sun-Earth system.

Some important results regarding the movement of a “test particle” under the action of the gravitational field of two massive bodies within our solar system have been presented in our previous work (Hysa, 2016, Hysa, Klemo, Xhomara, 2016).

4. Conclusion

The path to the Lagrange points, to send space telescopes there, is very important and a current challenge for scientists. In this paper we study a scarcely explored field of Celestial Mechanics and Astrodynamics. The main contribution of this study was to construction periodic orbits around the Lagrange Points (LP) L_1, L_2 and Invariant Manifolds within the Earth-Moon system. The problem we considered has to do with the relative movement of an astronomical test object. The movement of this object is described by a non-linear dynamic and its study is quite difficult and complex because such dynamics has a very high sensitivity to the initial conditions of the problem. But, we can study the behavior of this system from various initial conditions of coordinates and velocities.

References

Belbruno, E., Gidea, M., and Topputo, F. (2010). WEAK STABILITY BOUNDARY AND INVARIANT MANIFOLDS, http://dx.doi.org/10.1137/090780638.

Curtis H. D. (2014). Orbital Mechanics for Engineering Students Third Edition. Copyright 2014 Elsevier Ltd. ISBN–13: 978-0-08-097747-8.

Fehlberg E. (1960). Neue genauere Runge-Kutta-Formeln für Differentialgleichungenn-ter Ordnung. Z. Angew. Math. Mech.40, 449–455.

Fehlberg E. (1968). Classical Fifth-, Sixth-, Seventh-, and Eighth-Order Runge-Kutta Formulas with Stepsize Control. NASA TR R-287.

Fehlberg E. (1969). Low-Order Classical Runge-Kutta Formulas with Stepsize Control and their Application to some Heat Transfer Problems. NASA TR R-3 15.

Hysa, A. (2016). Numerical study of the linear and nonlinear dynamics near L_1 and L_2 points in the Earth-Moon system. International Journal of Current Research, ISSN: 0975-833X, Vol. 8, Issue, 01, pp.25289-25294, January, 2016. https://www.journalcra.com/article/numerical-study-linear-and-nonlinear-dynamics-near-l1-and-l2-points-earth-moon-system

Hysa, A., Klemo, M., Xhomara, I. (2016). Dynamics of Celestial Bodies. Online International Interdisciplinary Research Journal, ISSN 2249-9598, Volume-VI, Nov 2016 Special Issue (1). pp: 85-91. http://oiirj.org/oiirj/blog/2016/11/24/vol-vi-nov2016-special-issue-1/
Jacobi C. G. J. (1836). Comptes Rendus de l’Acad´emie des Sciences de Paris, 59.

James J. D. M. (2006). Celestial Mechanics Notes Set 4: The Circular Restricted Three Body Problem. https://cosweb1.fau.edu/~jmirelesjames/hw4Notes.pdf.

Jing Lu, Qishao Lu, and Qi Wang. A station-keeping strategy for collinear libration point orbits. Theoretical & Applied Mechanics Letters 1, 033002 (2011). doi:10.1063/2.1103302.

Lagrange J. L. (1772). "Essai sur le Problème des Trois Corps," Oeuvres de Lagrange, Vol. 6, pp. 229-292. Paris: Gauthier-Villars, 1873.

More A., Ober-Blöbaum S., & Marsden J., E., (2012). Trajectory Design Combining Invariant Manifolds with Discrete Mechanics and Optimal Control. Journal of Guidance, Control, And Dynamics Vol. 35, No. 5, September–October 2012.

Newton I. (1687). Philosophiæ naturalis principia mathematica (Mathematical Principles of Natural Philosophy). London: Royal Society Press.

Parker J. S., Anderson, R. L. (2013). Low-energy lunar trajectory design. https://descanso.jpl.nasa.gov/monograph/series12/LunarTraj--Overall.pdf.

Poincaré, J. H. (1890). Sur le probleme des trois corps et les equations de la dynamique. Divergence des series de m. Lindstedt, Acta Math. 13, 1–270.

Runge, C, "Ueber die numerishe Auflosung von DifTerentialgleichungen," Math. Ann., Vol. 46, pp. 167-178.

Strogatz S. H. (1995). Nonlinear Dynamics and Chaos with applications to physics, biology, chemistry, and engineering", Addison wesley, Reading MA G.L. ISBN 0-201-54344-3.

Szebehely, V. (1967). Theory of Orbits: The Restricted Problem of Three Bodies, Academic Press, New York, 1967.

Thurman R., Worfolk P. A. (1996). The geometry of halo orbits in the circular restricted three-body problem. The Geometry Center, University of Minnesota 1300 S. Second St., Suite 500 Minneapolis, MN, 554554.

Trusdale, N. (2012). Using Invariant Manifolds of the Sun-Earth L2 Point for Asteroid Mining Operations. ASEN 5050 Spaceflight Dynamics 12/19/2012.

Utku A. (2013). Low-cost capture using multi-body dynamics. UNIVERSITY OF SURREY Surrey Space Centre School of Electronics and Physical Sciences University of Surrey Guildford, Surrey, GU2 7XH, U.K. MAY.